

## Optimization, performance, and application of a pyrolysis-GC/MS method for the identification of microplastics

Hermabessiere Ludovic <sup>1</sup>, Himber Charlotte <sup>1</sup>, Boricaud Beatrice <sup>1</sup>, Kazour Maria <sup>2,3</sup>, Amara Rachid <sup>2</sup>, Cassone Anne-Laure <sup>4</sup>, Laurentie Michel <sup>5</sup>, Paul-Pont Ika <sup>4</sup>, Soudant Philippe <sup>4</sup>, Dehaut Alexandre <sup>1</sup>, Duflos Guillaume <sup>1,\*</sup>

<sup>1</sup> ANSES, Lab Securite Aliments, Blvd Bassin Napoleon, F-62200 Boulogne, France.

<sup>2</sup> Univ Lille, Univ Littoral Cote Opale, CNRS, UMR 8187,LOG, 32 Ave Foch, F-62930 Wimereux, France.

<sup>3</sup> CNRS, Natl Ctr Marine Sci, POB 534, Batroun, Lebanon.

<sup>4</sup> UBO, IFREMER, CNRS, UMR6539,IRD,Lab Sci Environm Marin LEMAR,Inst Uni, Technopole Brest Iroise,Rue Dumont Urville, F-29280 Plouzane, France.

<sup>5</sup> ANSES, Plateforme PAS, Lab Fougeres, 10 B Rue Claude Bourgelat, F-35300 Fougeres, France.

\* Corresponding author : Ludovic Hermabessiere, email address : [guillaume.duflos@anses.fr](mailto:guillaume.duflos@anses.fr)



### Abstract :

Plastics are found to be major debris composing marine litter; microplastics (MP, < 5 mm) are found in all marine compartments. The amount of MPs tends to increase with decreasing size leading to a potential misidentification when only visual identification is performed. These last years, pyrolysis coupled with gas chromatography/mass spectrometry (Py-GC/MS) has been used to get information on the composition of polymers with some applications on MP identification. The purpose of this work was to optimize and then validate a Py-GC/MS method, determine limit of detection (LOD) for eight common polymers, and apply this method on environmental MP. Optimization on multiple GC parameters was carried out using polyethylene (PE) and polystyrene (PS) microspheres. The optimized Py-GC/MS method require a pyrolysis temperature of 700 °C, a split ratio of 5 and 300 °C as injector temperature. Performance assessment was accomplished by performing repeatability and intermediate precision tests and calculating limit of detection (LOD) for common polymers. LODs were all below 1 µg. For performance assessment, identification remains accurate despite a decrease in signal over time. A comparison between identifications performed with Raman micro spectroscopy and with Py-GC/MS was assessed. Finally, the optimized method was applied to environmental samples, including plastics isolated from sea water surface, beach sediments, and organisms collected in the marine environment. The present method is complementary to µ-Raman spectroscopy as Py-GC/MS identified pigment containing particles as plastic. Moreover, some fibers and all particles from sediment and sea surface were identified as plastic.

## Graphical abstract

### 1. Optimization



PE  and PS 

Pyrolysis temperature: 700 °C

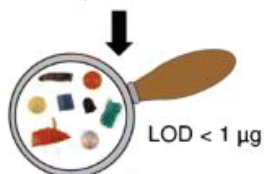
Split ratio: 5

Injector temperature: 300 °C

### 2. Validation

✓ Repeatability

Intermediate precision



µ-Raman



### 3. Application

Particles from:



% Identification: - Pigment: 70 %  
- Fiber: 20 %  
- Fragment: 100 %

**Keywords** : Microplastics, Pyrolysis, Gas chromatography, Method, Environmental samples

## 47 **1. Introduction**

48 Plastic is a commonly used material as it is inexpensive, strong, lightweight, and easy to  
49 manufacture [1]. Plastic production increased from the 1950's and reached 335 million metric  
50 tons in 2016 [2]. Due to waste management issues and incivilities, it has been estimated that 5  
51 to 12 million plastic particles end up in Oceans in 2010 [3]. Low estimates predicted that  
52 floating marine plastic weight between 70,000 and 270,000 tons [4-6], thus, potentially  
53 representing more than 51 trillion plastic pieces in Oceans [6].

54 Microplastics (MP) are plastic particles smaller than 5 mm in their longest size [7]. To date,  
55 multiple studies are carried out to quantify MP in sediments, in water column, and in  
56 organisms from both freshwater and marine environments [8, 9]. For large MP (1-5 mm) [10]  
57 and macroplastic (>5 mm), visual identification relying on physical characteristics is possible  
58 but the proportion of misidentification grows with decreasing particles size [11]. However,  
59 some studies still do not perform any characterization of MP based on their chemical  
60 composition [12]. Additionally, as plastic materials include a large variety of polymers, more  
61 than 5,000 grades [13], chemical identification is now mandatory to ensure the accuracy of  
62 collected pollution data [14]. Raman and Fourier-Transform Infrared (FTIR) spectroscopies  
63 are the most common techniques employed to identify polymer types of MP [15].  
64 Furthermore, the use of imaging techniques coupled to spectroscopic approaches allows  
65 automatization of MP identification [16-18]. In addition to spectroscopic methods, another  
66 type of chemical identification is thermal analysis [12]. Pyrolysis-Gas Chromatography  
67 coupled with Mass Spectrometry (Py-GC/MS) is one of the thermal analysis techniques used  
68 to identify MP polymers. Py-GC/MS has been used to identify MP from different matrix  
69 based on their thermal degradation products [19-25]. Furthermore, Py-GC/MS allows the  
70 analysis of a whole MP particle in contrast with Raman or FTIR (in reflection mode) which

71 only analyze the surface of the MP particle being sensitive to interference caused by additives  
72 such as pigments [26-28], for example.

73 To date, studies using Py-GC/MS to identify the polymeric composition of MP document  
74 neither the method development nor the assessment of its performance. Some authors stated  
75 that Py-GC/MS is only feasible with MP >500  $\mu\text{m}$  [29, 30] even if so far, 100  $\mu\text{m}$  is the  
76 smallest size of an isolated MP that has been identified [19]. Recently, particles smaller than 1  
77  $\mu\text{m}$ , referred as nanoplastics by the authors, have been identified as plastics based on Py-  
78 GC/MS and statistical approaches in bulk samples from the North Atlantic Subtropical Gyre  
79 [31].

80 The purpose of this work was fourfolds: (i) optimize a Py-GC/MS method to accurately  
81 identify polymer of MP, (ii) assess the performance of the Py-GC/MS approach, (iii) compare  
82 identifications with samples already identified by  $\mu$ -Raman and (iv) apply this technique to  
83 environmental samples.

## 84 **2. Material and methods**

### 85 **2.1. Reference material**

86 Microspheres with calibrated size ranges were purchased for the Py-GC/MS optimization  
87 method. Polyethylene (PE) (180-212  $\mu\text{m}$ ; reference: CPMS-0.96 180-212 $\mu\text{m}$ ) and  
88 Poly(Methyl Methacrylate) (PMMA) (180-212  $\mu\text{m}$ ; reference: PMMAMS-1.2 180-212 $\mu\text{m}$ )  
89 microspheres were acquired from Cospheric LLC (Santa Barbara, USA) and Polystyrene (PS)  
90 (106-125  $\mu\text{m}$ ; reference: 198241) from Polysciences Europe GmbH (Hirschberg an der  
91 Bergstrasse, Germany). For the calculation of the LOD, other polymers were bought from  
92 Goodfellow (Lille, France) including filaments of polycaprolactam (PA-6), polyethylene

93 terephthalate (PET) and polypropylene (PP) and fragments of polycarbonate (PC) and  
94 unplasticized polyvinyl chloride (uPVC).

95 For all polymers, characteristic compounds are presented in Table 1 (see Electronic  
96 Supplementary Material Figure S1 to S8) and were choose according to their  
97 representativeness for polymer identification, their relative intensity, and in comparison with  
98 the literature [22, 32, 33].

99

100 **Table 1 Polymer related pyrogram information**

Polymer	Characteristic compound <sup>a</sup>	LRI <sup>b</sup>	Indicator ion (m/z)
PE	1-Nonene (C9)	893	83; 97
	<b>1-Decene (C10)</b>	993	83; 97
	1-Undecene (C11)	1093	83; 97
	1-Dodecene (C12)	1192	83; 97
	1-Tridecene (C13)	1292	83; 97
	1-Tetradecene (C14)	1392	83; 97
	1-Pentadecene (C15)	1492	83; 97
	1-Hexadecene (C16)	1578	83; 97
PS	<b>Styrene</b>	898	78; 104
	3-butene-1,3-diylidibenzene (styrene dimer)	1733	91; 208
PMMA	<b>Methyl methacrylate</b>	743	41; 69; 100
PP	<b>2;4-dimethyl-1-heptene</b>	846	70
PA-6	<b><math>\epsilon</math>-caprolactam</b>	1274	113
PC	Phenol	980	66; 94
	p-Cresol	1075	77; 107
	p-Ethylphenol	1168	107; 122
	p-Vinylphenol	1217	91; 120
	<b>p-Isopropenylphenol</b>	1304	119; 134
	Bisphenol A	2088	213; 228
PET	Benzene	770	52; 78
	<b>Acetophenone</b>	1076	51; 77; 105
	Vinyl benzoate	1145	52; 77; 105
	Benzoic acid	1178	77; 105; 122
	Divinyl terephthalate	1574	104; 175
uPVC	Benzene	770	52; 78
	Toluene	782	91
	Styrene	898	78; 104
	Indene	1059	116
	<b>Naphthalene</b>	1206	128
	2-methylnaphthalene	1320	115; 142
	1-methylnaphthalene	1340	115; 142

<sup>a</sup> Marker compounds in bold were used to calculate Limit of Detection;

<sup>b</sup> Retention Index were calculated according to [van Den Dool and Kratz \[34\]](#); m/z: mass to charge ratio

101 **2.2. Sample preparation**

102 Each particle was selected based on its size (*ca.* 200  $\mu\text{m}$ ) under a SZ61 stereomicroscope  
103 (Olympus, Rungis, France) and then introduced into an analysis cup (Frontier-Lab,  
104 Fukushima, Japan) for Py-GC/MS analysis. All analysis cup used in this work were brand  
105 new cups visually controlled prior to analysis to detect any possible contamination.

106 **2.3. Size and weight estimation**

107 In order to estimate the size of the particle, a photograph was taken with a scale bar using a  
108 DP21 camera (Olympus, Rungis, France) mounted on the stereomicroscope. The size in pixel  
109 of the particle was recorded using GIMP 2 software (2.8.16). Then, the maximum size in  $\mu\text{m}$   
110 of the particle was calculated using the scale bar. For each particle, the volume ( $\text{cm}^3$ ) was  
111 estimated using different formula (1), (2) or (3), where D corresponds to the diameter, L to the  
112 length and S to the side size (see Electronic Supplementary Material Weight estimation). The  
113 volume was then multiplied by the density ( $\text{g}/\text{cm}^3$ ) of the polymer to obtain the estimated  
114 weight.

$$(1) \textit{Microsphere volume} = \frac{4}{3} \times \pi \times \left(\frac{D}{2}\right)^3$$

$$(2) \textit{Filament volume} = \left(\frac{D}{2}\right)^2 \times \pi \times L$$

$$(3) \textit{Fragment volume} = S^2 \times L$$

115 **2.4. Method optimization**

116 **2.4.1. Initial Py-GC/MS method**

117 The hereafter called “initial method” was described by [Dehaut et al. \[35\]](#). Briefly, the analysis  
118 cup containing the plastic was placed on the AS-1020E autosampler of an EGA/PY-3030D  
119 device (Frontier Lab, Fukushima, Japan). Samples were pyrolysed at 600  $^{\circ}\text{C}$  for 1 min.

120 Pyrolysis products were injected with a split of 20, on a GC-2010 device (Shimadzu, Noisiel,  
121 France) equipped by a Rxi-5ms® column (60 m, 0.25 mm, 25 µm thickness) (Restek, Lisses,  
122 France). Temperatures of the pyrolyzer interface and the injection port were both set at 300  
123 °C. Helium was used as a carrier gas with a linear velocity of 40 cm/s. The initial oven  
124 program, called here after **program 0**, was set as follows: 40 °C for 2 min, then increase to  
125 320 °C at 20 °C/min, maintained for 14 min. Mass spectra were obtained by a Shimadzu  
126 QP2010-Plus mass spectrometer. Interface temperature was set at 300 °C, ion source  
127 temperature was set at 200 °C, ionization voltage was set at 70 eV, and a mass range from 33  
128 to 500 m/z was scanned at 2000 Hz.

129 As a primary attempt, polymer identification was realized using total ion pyrogram (TIC)  
130 which was firstly identified using F-Search software 4.3, querying pyrograms against Frontier  
131 Lab's database, and our own database containing pre-established pyrograms with plastic  
132 samples. Identification was established based on the similarity percentage (minimum value of  
133 80%) between average mass spectra on the whole chromatogram. Our home-made database  
134 was created using our “initial method” and the optimized Py-GC/MS method on plastic  
135 references from Goodfellow (Lille, France). Plastic references used for our home-made  
136 database included: PE, PS, PP, PET, PA-6, PC, PMMA and uPVC.

137 When identification was not possible after primary attempt, a classical GC/MS treatment was  
138 performed. Peaks of pyrograms were integrated and compared with available literature [32] or  
139 characteristic compounds (Table 1), single peak identification being carried out using NIST08  
140 database and LRI.



141 **2.4.2. Pyrolysis temperature**

142 Optimization of the pyrolysis temperature was carried out using the initial pyrolysis method.

143 The impact of pyrolysis temperature was determined using five replicate of PE microspheres.

144 Three additional pyrolysis temperatures were tested: 500, 700 and 800 °C for 1 min.

145 **2.4.3. GC oven temperature program**

146 In addition to **Program 0**, two others temperature programs were tested. **Program 1** was set

147 as follow: 40 °C for 2 min, then increase to 200 °C at 15 °C/min followed by a second

148 increase to 300 °C at 10 °C/min maintained for 2 min. **Program 2** was set as follow: 40 °C

149 for 2 min, then increase to 261 °C at 13 °C/min followed by a second increase to 300 °C at 6

150 °C/min maintained for 2 min. Except pyrolysis temperature was set at 700 °C the optimal

151 temperature for 1 min (*cf.* 3.1.1), oven program was the unique parameter modified in this

152 part, other parameters were conserved as those of the initial method. The impact of GC oven

153 temperature program on resolution was determined using PE microspheres. Here the

154 resolution was only used to assess the separation between PE alkene and alkadiene. The

155 resolution of alkenes (from C<sub>9</sub> to C<sub>16</sub>) was used to evaluate each program performance.

156 Resolution was calculated by the Shimadzu GC-MS postrun analysis software using (4),

157 where T<sub>r</sub> corresponds to the retention time of the considered peak (Alkene), T<sub>rp</sub> to the

158 retention time of the previous peak (Alkadiene), W to the width of the considered peak and

159 W<sub>p</sub> to the width of the previous peak:

$$(4) \text{ Resolution} = 2 \times \frac{T_r - T_{rp}}{W + W_p}$$

160 Five replicates were performed per programs.

#### 161 **2.4.4. Injector temperature and split ratio**

162 Optimization on the split ratio and injector temperature was performed using PE and PS  
163 microspheres. Here, PS was used in addition to PE as this polymer exhibits only a few  
164 degradation products after pyrolysis (Table 1). Three split ratios (50, 20 and 5) and three  
165 injector temperatures (280, 300 and 320 °C) were applied, resulting in nine distinct  
166 combinations. For all combinations, pyrolysis temperature and GC oven program were set  
167 following the previous optimization steps, others parameters were conserved as those  
168 described for the initial method (*cf.* 2.4.1). For each combination, five microspheres of PE and  
169 PS were analyzed.

#### 170 **2.5. Method performance evaluation**

171 Split ratios were adjusted to ensure that no saturation of the mass spectrum occurred. To do so,  
172 split ratio was set at 5 for PE microspheres, particles identified by  $\mu$ -Raman spectroscopy, and  
173 unknown particles injection, whereas for PMMA and PS microspheres injection, a split of 50  
174 was chosen.

##### 175 **2.5.1. Repeatability and intermediate precision**

176 For repeatability and intermediate precision, respectively ten and five microspheres of the  
177 three polymers were pyrolysed and the Relative Standard Deviation (RSD) (5) was calculated  
178 for each characteristic peak according to ISO 5725-3 [36] where  $s$  is the standard deviation  
179 and  $m$  is the mean:

$$(5) RSD (\%) = \frac{s}{m} \times 100$$

180 Intermediate precision was assessed over time with pyrolysis occurring at 3, 4 and 6 weeks  
181 after repeatability experiences. The method is considered valid if RSD is below 20 % for  
182 repeatability and intermediate precision. Moreover, polymer identification of the particles was  
183 performed as previously described (*cf.* 2.4.1) to obtain qualitative data.

184 **2.5.2. Limit of detection**

185 Limit of detection was calculated according to [Caporal-Gautier et al. \[37\]](#). First, ten analysis  
186 cups without plastic, hereafter referred as “blank”, were pyrolysed. For each blank and at the  
187 retention time of each characteristic peak of the eight used polymers (Table 1), the maximum  
188 height was determined over a time interval equal to 20 times the full width at half maximum  
189 (FWHM), this area is called  $H_{20FWHM}$ . Interval surrounds the retention time of each peak with  
190 the retention time being the central point of the time range. Five particles were pyrolysed for  
191 each polymer. A response factor (R) (6) was calculated: “Weight” corresponds to the mean  
192 the average calculated weight and “Height” corresponds to the mean height of the  
193 characteristic peak for the five particles:

$$(6) \text{ Response factor } (R) = \frac{\text{Weight}}{\text{Height}}$$

194 Finally, for each polymer LOD were calculated as follow:

$$(7) \text{ Limit of Detection } (LOD) = 3 \times R \times H_{20FWHM}$$

195 **2.6. Method comparison**

196 **2.6.1. Sampling**

197 Unknown plastic particles were first analysed by  $\mu$ -Raman and then by Py-GC/MS before  
198 identification to be compared. Comparison of the identification of unknown plastic particles  
199 obtained after  $\mu$ -Raman spectroscopy and Py-GC/MS was performed. To assess methods  
200 comparison, fifty plastic particles hand sampled on a local beach (Equihen Plage, France –  
201 50°39'51.08"N, 1°34'17.94"E) were used.

202 **2.6.2. Identification by  $\mu$ -Raman and Py-GC/MS**

203 For  $\mu$ -Raman analysis, each particle was analyzed with an XploRA PLUS V1.2 (HORIBA  
204 Scientific, France SAS) equipped with two lasers of 785 and 532 nm wavelength. First, plastic

205 particles were analyzed with laser wavelength set at 785 nm over a range of 50 to 3,940  $\text{cm}^{-1}$   
206 with a x10 (NA=0.25; WD=10.6 mm) or x100 (NA=0.9; WD=0.21 mm) objective (Olympus,  
207 France). If identification with the 785 nm laser was not successful, particles were secondly  
208 analyzed with a laser wavelength set at 532 nm over a range of 50 to 4,000  $\text{cm}^{-1}$  with a x10 or  
209 x100 objective. The experimental conditions (integration time, accumulation, laser power)  
210 were adapted to limit fluorescence and increase the spectral quality of the analyzed particles.  
211 Polymer identification was carried out using spectroscopy software (KnowItAll, Bio-Rad) and  
212 our own database containing pre-established polymers spectra. Identification was considered  
213 correct if Hit Quality Index (HQI) was above 80 (ranging from 0 to 100). If identification of a  
214 particle was not successful after  $\mu$ -Raman spectroscopy, the particle was then included in the  
215 section 2.7.

216 For Py-GC/MS, a piece of each particle was cut to the smallest possible size and prepared as  
217 indicated in section 2.2. Pyrolysis-GC/MS was realized as described above (*cf.* 2.5).

## 218 **2.7. Application: identification of unknown particles**

### 219 **2.7.1. Sampling**

220 Application of the Py-GC/MS was performed using particles collected on a beach, extracted  
221 from bivalves and collected on sea surface waters.

222 Ten particles, collected by hand on a local beach, including 4 particles identified as pigment  
223 and 6 particles unidentified (*cf.* 3.3) were analyzed using Py-GC/MS.

224 Mussels (*Mytilus edulis*) and cockles (*Cerastoderma edule*) were respectively sampled during  
225 morning low tides at Le Portel, France (50°42'30.02"N, 1°33'34.43"E) on 10/29/2015 and at  
226 Baie d'Authie, France (50°22'17.22"N, 1°35'4.8"E) on 11/15/2015. Bivalves were then  
227 dissected, digested, and filtered using the method of [Dehaut et al, \[35\]](#). Particles resembling  
228 plastic found in bivalves were extracted under a stereomicroscope using tweezers and

229 submitted to  $\mu$ -Raman identification using an LabRam HR800 (HORIBA Scientific,  
230 Villeneuve d'Ascq, France) following a methodology adapted from Frère et al, [16]. Here, 16  
231 particles from bivalves, previously identified as pigments containing particles, and 10  
232 unknown particles in form of fibers were analyzed. Finally, 24 unknown particles collected in  
233 sea-surface trawls from the bay of Brest, as described by Frère et al. [38], were used for  
234 identification by Py-GC/MS.

### 235 **2.7.2. Identification by Pyrolysis-GC/MS**

236 In total, sixty particles with no previous polymer identification were analyzed. For Py-  
237 GC/MS, a piece of each particle was cut to the smallest size possible and prepared as  
238 indicated in section 2.2. Pyrolysis-GC/MS was realized as described above (*cf.* 2.5). Results  
239 will be present and discuss according to the following categories: pigments containing  
240 particles, fibers and others particles.

### 241 **2.8. Statistical analyses**

242 All statistical analyses with an exception for RSD calculation were performed using R (3.4.0)  
243 [39]. For method optimization, including verification of estimated size of microspheres used,  
244 normality and homoscedasticity of the distribution hypothesis were carefully verified before  
245 performing ANOVA. Assuming one of the hypothesis was not verified, a Kruskal-Wallis test  
246 was carried out. Kruskal-Wallis tests were followed by a conservative post-hoc test using the  
247 Fisher's least significant difference (LSD) criterion and Bonferroni correction. Post-hoc tests  
248 were performed using the agricolae package (1.2-7) [40]. All results are expressed as a mean  
249  $\pm 2$  standard error (S.E), representing the 95% confidence interval (95% CI). Differences were  
250 considered significant when  $p$ -value $<0.05$ . On bar charts, two different letters illustrates  
251 significantly different value with a 95% CI.

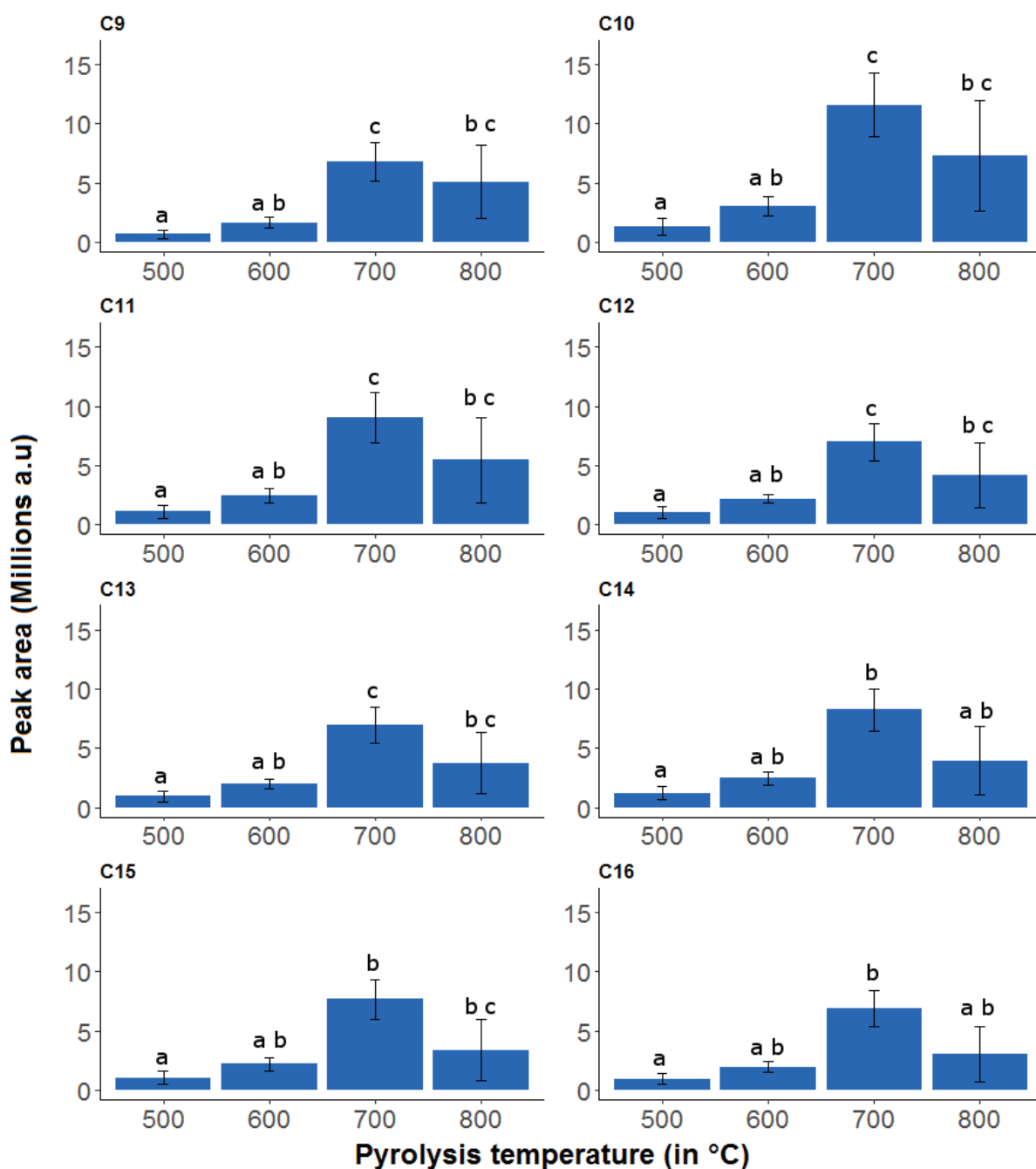
### 252 **3. Results and discussion**

253 All procedural blank, *i.e* analysis cup without sample, presented no sign of contamination by  
254 pyrolytic products of synthetic polymers.

#### 255 **3.1. Method optimization**

##### 256 **3.1.1. Pyrolysis temperature**

257 PE microspheres size (204 to 214  $\mu\text{m}$ ) used for optimizing the pyrolysis temperature were not  
258 significantly different for each tested temperatures (One-way ANOVA,  $p>0.05$ ). Pyrolysis  
259 temperature (500, 600, 700 and 800  $^{\circ}\text{C}$ ) had a significant impact on the peaks areas of PE  
260 (Fig. 1). On the one hand, for the eight characteristic compounds of PE, peaks areas rises  
261 when the pyrolysis temperature increase from 500 to 700  $^{\circ}\text{C}$  but on the other hand at 800  $^{\circ}\text{C}$ ,  
262 peaks areas slightly decreased (Fig. 1). Moreover, significant difference of areas were  
263 recorded for characteristic compounds of PE (Kruskal-Wallis,  $p<0.05$ ). Areas were  
264 significantly higher at 700  $^{\circ}\text{C}$  in comparison with areas at 500  $^{\circ}\text{C}$  (Kruskal-Wallis followed  
265 by post-hoc,  $p<0.05$  – Fig. 1). Significant differences between areas at 600 and 700  $^{\circ}\text{C}$  were  
266 observed for 1-Nonene, 1-Decene, 1-Undecene, 1-Dodecene, and 1-Tridecene (Kruskal-  
267 Wallis followed by post-hoc,  $p<0.05$  – Fig. 1). However, no significant difference was  
268 observed between 500 and 600  $^{\circ}\text{C}$ , between 700 and 800  $^{\circ}\text{C}$ , and between 600 and 800  $^{\circ}\text{C}$  for  
269 all 8 characteristics compounds (Kruskal-Wallis followed by post-hoc,  $p<0.05$  – Fig. 1). At  
270 800  $^{\circ}\text{C}$ , pyrograms of PE microspheres were not all typical with the presence of unknown  
271 compounds at the beginning of the pyrogram which lead to identification with a percentage  
272 below 80 % (see Electronic Supplementary Material Figure S9). As 700  $^{\circ}\text{C}$  demonstrated  
273 higher areas for characteristic compounds of PE with typical and clearly identified pyrograms;  
274 optimal pyrolysis was then set at 700  $^{\circ}\text{C}$ .



275

276 Fig. 1 Peaks areas (Arbitrary Unit) depending on the Pyrolysis temperature (in °C) for eight characteristic  
 277 compounds of PE. Values as expressed as mean  $\pm$  95 % confidence interval. Letters correspond to the  
 278 differences after post-hoc test using the Fisher's least significant difference with Bonferroni correction.  
 279 C9: 1-Nonene; C10: 1-Decene; C11: 1-Undecene; C12: 1-Dodecene; C13: 1-Tridecene; C14: 1-  
 280 Tetradecene; C15: 1-Pentadecene; C16: 1-Hexadecene

281 Regarding the literature, studies generally used a pyrolysis temperature of 700 °C [19-21, 23,

282 31, 33] while others used lower temperature such as 550 °C [24], 590 °C [22], 600 °C [32, 35]

283 or 650 °C [25]. As presented in this work, pyrolysis temperature had a clear impact on the

284 signal of the pyrolytic products of PE and could potentially impact identification for small

285 particles. Additionally, pyrolysis at a temperature greater than or equal to 800 °C had a  
286 negative effect on PE pyrolytic products. Indeed, the signal was decreased and the polymer  
287 identification was not possible with our software due to the presence of a large interfering  
288 peak at the beginning of the pyrogram (see Electronic Supplementary Material Figure S9).  
289 Moreover, as indicated by Kusch [33], pyrolysis temperature could also impact the generated  
290 pyrolysis products. Here for PC, PET, and uPVC some pyrolysis products were different from  
291 those recorded with the initial Py-GC/MS method [35] and from a reference book [32]. Such  
292 differences could prevent identification of these polymers as many libraries were obtained  
293 after pyrolysis at 600 °C. However, the use of our own database create with pyrolysis  
294 temperature set at 700 °C allow accurate polymer identification.

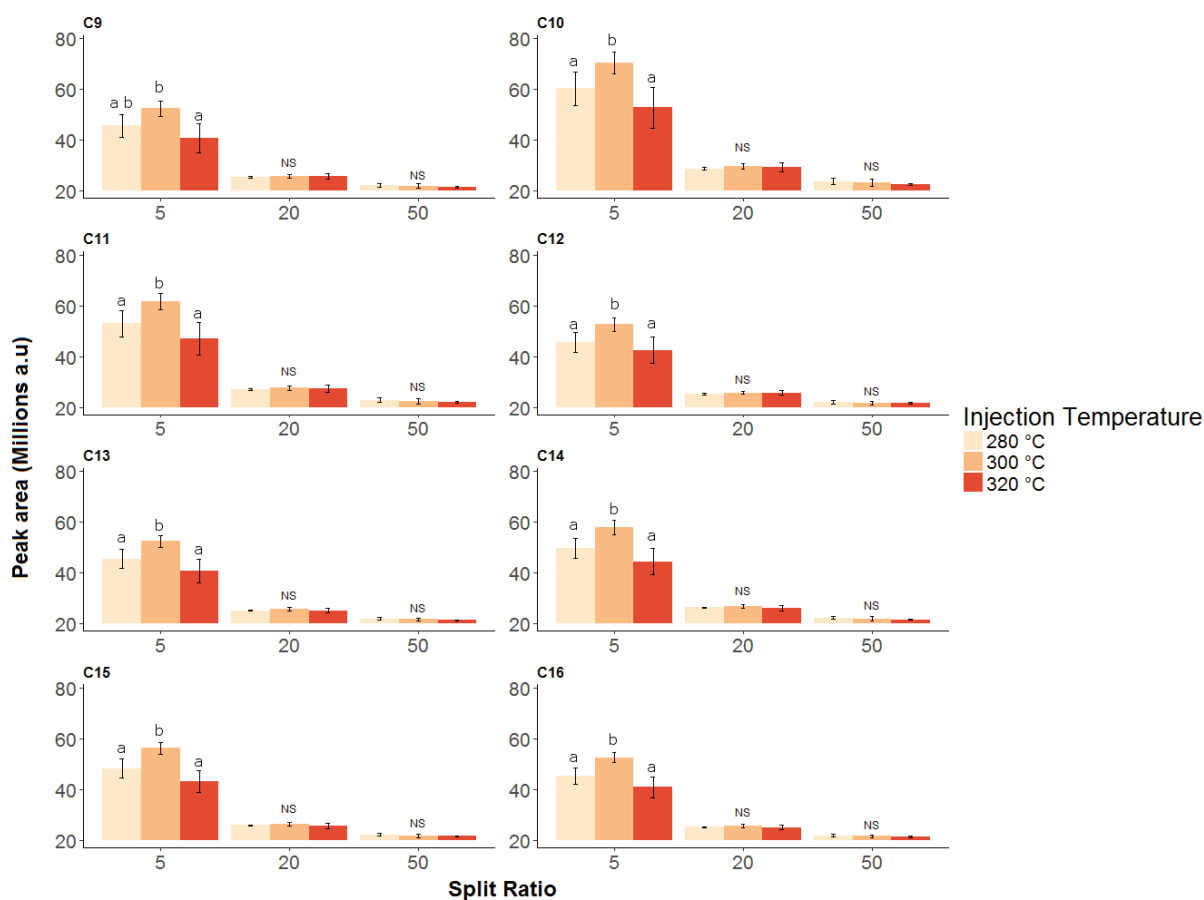
### 295 **3.1.2. GC oven temperature program**

296 PE microspheres size (197 to 226 μm) used for the optimization of the GC oven temperature  
297 program were not significantly different for each tested conditions (One-way ANOVA,  
298  $p>0.05$ ). For all characteristic compounds of PE and for the three GC oven temperature  
299 programs, resolution was above 1.5 (see Electronic Supplementary Material Figure S10)  
300 which is acceptable [41]. Significant differences in resolution were observed for all peaks of  
301 PE (Kruskal-Wallis,  $p<0.01$ ) depending on the used GC oven temperature program.  
302 Moreover, program 2 demonstrated higher resolution in comparison with program 0 and 1  
303 (Kruskal-Wallis followed by Fisher's LSD with Bonferroni correction,  $p<0.05$  – see  
304 Electronic Supplementary Material Figure S10). Here, resolution and peak separation was  
305 higher when ramping temperature decrease. Higher peak resolution could be useful for  
306 manual identification of peaks, if primary attempt using F-Search software is not conclusive.  
307 Program 2 was then applied to perform separation of pyrolysis compounds using the GC  
308 system.



309 **3.1.3. Injector temperature and split ratio**

310 PS (110 to 136  $\mu\text{m}$ ) and PE (188 to 223  $\mu\text{m}$ ) microspheres size used for the optimization on  
311 split ratio and injection temperature were not significantly different for each tested conditions  
312 (One-way ANOVA,  $p>0.05$ ). For all characteristic compounds of PE, areas significantly  
313 decreased with the increase of split ratio (Kruskal-Wallis followed post-hoc,  $p<0.05$  – Fig. 2).  
314 Moreover, no significant difference in peaks areas were observed at split ratio of 20 and 50  
315 depending on the injector temperature used (Kruskal-Wallis,  $p>0.05$ ). However, it should be  
316 noticed that significant differences between injection at 280, 300, and 320  $^{\circ}\text{C}$  were observed  
317 using a split ratio of 5 for all characteristic compounds (Kruskal-Wallis followed by post-hoc,  
318  $p<0.05$  – Fig. 2). Indeed, with the exception of 1-Nonene, the highest peaks areas were  
319 obtained when injector temperature was set at 300  $^{\circ}\text{C}$  with a split ratio of 5 (Fig. 2).



320  
321 **Fig. 2 Peaks areas (Arbitrary Unit) depending on the split ratio and injection temperature for 8**  
322 **characteristics compounds of PE. Values as expressed as mean  $\pm$  95 % confidence interval. Letters**

323 correspond to the differences after post-hoc test using the Fisher's least significant difference with  
324 Bonferroni correction and NS stand for non-significant. C9: 1-Nonene; C10: 1-Decene; C11: 1-Undecene;  
325 C12: 1-Dodecene; C13: 1-Tridecene; C14: 1-Tetradecene; C15: 1-Pentadecene; C16: 1-Hexadecene

326 For PS, as for PE, increasing split ratio decreased peaks areas (Kruskal-Wallis,  $p < 0.01$  – see  
327 Electronic Supplementary Material Figure S11). For styrene, at a split ratio of 5, areas were  
328 significantly different between 320 °C and the others temperatures (Kruskal-Wallis followed  
329 by post-hoc,  $p < 0.05$  – see Electronic Supplementary Material Figure S11) and at a split ratio  
330 of 20, areas were significantly different between 280 and 320 °C (Kruskal-Wallis followed by  
331 post-hoc,  $p < 0.05$  – see Electronic Supplementary Material S11). However, no significant  
332 difference were observed for area values at a split ratio of 50 between injector temperatures  
333 (Kruskal-Wallis,  $p < 0.05$ ). No significant difference were observed for styrene dimer areas  
334 between injector temperatures at each split ratio (Kruskal-Wallis,  $p > 0.05$ ).

335 As split ratio is inversely related to the amounts of sample entering the column, such results  
336 were expected. Generally, studies using Py-GC/MS to identify MP used low split ratio to  
337 increase analyte signal. Indeed, splitless mode was used for injection by several authors [19-  
338 21, 24] while split ratio of 10 [25] or 15 [22] were used by others authors. In several works,  
339 split ratio was adapted depending on the weight of the particle to identify [24, 31]. Indeed, Ter  
340 Halle et al, [31] used a split ratio of 5 for nanoplastics (25 mg of lyophilizate), 10 for  
341 micrometric plastic (particle on filter) and 100 for meso and microplastics and commercial  
342 plastics (approximately 10 µg). In addition, in their work Hendrickson et al, [24] used the  
343 splitless mode for particles <20 µg and a split ratio of 100 for particles >20 µg. In the others  
344 studies few or no information are available on the size or the weight of MP used for Pyrolysis  
345 [19, 21, 22, 25]. Here, split ratios tested were between 5 and 50 to be around the split ratio  
346 used in our previous work [35] and in order to obtain area for PE characteristic peak above a  
347 million of arbitrary unit allowing correct identification using the software. With this  
348 optimized Py-GC/MS method, split ratio should also be adapted depending on the weight of

349 particles. Indeed, for unknown particles smaller than 5  $\mu\text{g}$  a split ratio of 5 should be used and  
350 for particles heavier than 5  $\mu\text{g}$ , split ratio should be set at 20. Moreover, injector temperature  
351 of 300 °C in combination with split ratio of 5 had a significant effect on peaks areas for all  
352 PE's peaks and for styrene from PS (Fig. 2 & see Electronic Supplementary Material Figure  
353 S11) which could be important to detect small particles. Here an injection temperature set at  
354 300 °C was chosen for performance assessment purpose.

355 Globally, method optimization is an important step for the detection and then the  
356 identification of MP using Py-GC/MS. Indeed, the higher the signal will be, the higher the  
357 probability of identification will be but mass spectrum saturation should be avoided to ensure  
358 proper identification. Moreover, MP signal tend to increase with an increasing size of the  
359 particle.

## 360 **3.2. Method performance evaluation**

### 361 **3.2.1. Method repeatability and intermediate precision**

362 PE, PMMA, and PS microspheres used for assessing method repeatability and intermediate  
363 precision did not display significant difference in sizes (One-way ANOVA or Kruskal-Wallis,  
364  $p>0.05$ ). Firstly, polymer identifications were, over the 6 weeks period, accurate with  
365 similarity percentage all above 90 %. Identification was successful in all cases and the method  
366 could be considered repeatable within a week and precise over the 6 weeks. Concerning the  
367 repeatability RSD, values were below 20 % for the characteristic compounds of PE and  
368 PMMA and above 20 % for characteristics compounds of PS (Table 2). For styrene dimer,  
369 highly variable peak areas were recorded for repeatability test. In addition RSD value above  
370 20% for styrene was due to one repetition that presents peak area 1.5 higher in comparison  
371 with others replicates. Then, concerning intermediate precision RSD values were above 20 %  
372 for all characteristics compounds of PE, PS, and PMMA (Table 2). Consequently, the method

373 is repeatable for PE and PMMA but not precise over time for all the three tested polymers,  
 374 regarding quantitative data. Depending on when the analysis was performed, a high variation  
 375 in peak areas was recorded and thus was responsible for high values of RSD. Indeed, at weeks  
 376 1, 3 and 4, areas of characteristics peaks were in the same order of magnitude (for an example  
 377 see see Electronic Supplementary Material Figure S12). However at week 6, an important  
 378 diminution of the signal was observed (see Electronic Supplementary Material Figure S12)  
 379 which can cause the high variability in RSD values for method intermediate precision.  
 380 Finally, despite a decrease over time in peaks areas for characteristic compounds of PE, PS  
 381 and PMMA, identifications remained exact. This is essential for future use of the optimized  
 382 Py-GC/MS method to identify MP.

383 **Table 2 Relative standard deviation (in %) for method repeatability (n=10) and intermediate precision**  
 384 **(n=20) for characteristics compounds of Polyethylene, Polystyrene and Poly(Methyl Methacrylate)**

<b>Polymer</b>	<b>Characteristic compound</b>	<b>Repeatability RSD (%)</b>	<b>Intermediate Precision RSD (%)</b>
PE	1-Nonene	10,67	31.82
	1-Decene	9,91	31.34
	1-Undecene	10,01	31.79
	1-Dodecene	9,55	31.40
	1-Tridecene	9,06	33.11
	1-Tetradecene	8,81	30.22
	1-Pentadecene	8,98	30.88
	1-Hexadecene	9,62	30.76
PS	Styrene	22,47	32.57
	3-butene-1,3-diylidibenzene (styrene dimer)	48,03	49.69
PMMA	Methyl methacrylate	9,19	24.34

385 **3.2.2. Limit of Detection**

386 The estimated LOD were below 1  $\mu\text{g}$  for all tested polymers using the optimized Py-GC/MS  
 387 (Table 3). Detection of smaller particles of polymers with a few peaks, such as PS or PMMA  
 388 could be easier compared to PE which presents numerous pyrolysis products.

389 **Table 3 Limit of detection (LOD) for eight common polymer and associate theoretical estimate size of**  
 390 **identifiable particle, in the form of sphere, fiber and fragment.**

Polymer	LOD (in $\mu\text{g}$ )	Theoretical size		
		Sphere diameter (in $\mu\text{m}$ ) <sup>d</sup>	Fiber length (in $\mu\text{m}$ ) <sup>d e</sup>	Fragment length (in $\mu\text{m}$ ) <sup>d f</sup>
PE <sup>a</sup>	0.070	51.7	229.9	28.9
PS <sup>a</sup>	0.003	17.7	9.2	1.2
PMMA <sup>a</sup>	0.029	35.9	77.2	9.7
PA-6 <sup>b</sup>	0.110	57.1	309.9	38.9
PP <sup>b</sup>	0.027	38.6	95.5	12.0
PET <sup>b</sup>	0.015	27.4	34.1	4.3
PC <sup>c</sup>	0.116	35.9	77.0	9.7
uPVC <sup>c</sup>	0.592	58.7	366.6	42.3

<sup>a</sup> Polymer used in form of microspheres; <sup>b</sup> Polymer used in form of filaments; <sup>c</sup> Polymer used in form of fragments; <sup>d</sup> LOD in size for sphere. fiber and fragment were calculated based on LOD in weight; <sup>e</sup> Calculation made with a diameter of 20  $\mu\text{m}$ ; <sup>f</sup> Calculation made based on a parallelepiped form with 50  $\mu\text{m}$  as side size.

391

392 To date, identification of isolated MP using Py-GC/MS was successful for particles with a  
 393 size down to 100  $\mu\text{m}$  [19] and down to 0.4  $\mu\text{g}$  [22]. Here, uPVC demonstrated the highest  
 394 LOD with 0.592  $\mu\text{g}$ . This could be explained by uPVC fragment form and important density.  
 395 Indeed, uPVC particles were thick ( $\approx$  310  $\mu\text{m}$ ) and long (195 to 220  $\mu\text{m}$ ) leading to heavy  
 396 particles ( $>$  20  $\mu\text{g}$ ) due to its important density (1.4  $\text{g cm}^{-3}$ ) leading to an heavy estimated  
 397 weight in comparison with other polymers. Globally, polymers with the highest densities, PA-  
 398 6, PC or uPVC, have the highest LOD (Table 3). In the present study, estimated weight of the  
 399 particles used for optimization and performance assessment were below 10  $\mu\text{g}$  with the  
 400 exception of uPVC particles and were even below 1  $\mu\text{g}$  for some polymers (*i.e.* PS and PP).  
 401 Furthermore, in previous works, Py-GC/MS was successfully applied to identify particles  
 402 weighting 20  $\mu\text{g}$  [24] and below 10  $\mu\text{g}$  [22]. Limit of detection expressed in  $\mu\text{g}$  were low and

403 demonstrate that this method is applicable to very small and light particles. In addition to  
404 LOD in  $\mu\text{m}$ , theoretical identifiable size (in  $\mu\text{m}$ ) were calculated for MP in form of spheres,  
405 fibers and fragments for all 8 polymer tested in the present study (Table 3). Those theoretical  
406 minimal identifiable sizes were calculated using the LOD expressed in mass, polymer density  
407 and equation (1-3) (see Electronic Supplementary Material Weight Estimation). For spheres,  
408 all identifiable size were below 60  $\mu\text{m}$  in diameter, for fibers of 20  $\mu\text{m}$  of diameter length size  
409 varied from 9.2  $\mu\text{m}$  to 366.6  $\mu\text{m}$  and for fragment all length size were below 50  $\mu\text{m}$  (Table 3).  
410 Here, these theoretical sizes showed that fiber are the MP form with the longest size  
411 identifiable with the optimized Py-GC/MS. Indeed, fibers are long but thin resulting in an  
412 important considered size (as the longest size was selected) with a low estimated weight.  
413 Moreover, as Py-GC/MS rely on particles weight, it is an important parameter to master in  
414 MP research.

415 MP are commonly defined as plastic particles smaller than 5 mm [7]. However, recently,  
416 some studies argue that plastic particles should be described using another parameter [42, 43].  
417 Here, as stated by [Simon et al, \[43\]](#), weight was chosen as an additional parameter to record  
418 during MP studies. Indeed, plastic including MP are three dimensions particles, the  
419 description of such particles accordingly to their longest size is problematic and could not be  
420 adequate for data interpretations [43]. Actually, it is easy to visualize that there is an  
421 important difference in weight for a fiber measuring 500  $\mu\text{m}$  in its longest size with few  
422 microns of diameters and a cubic fragment measuring 500  $\mu\text{m}$  for all its side. This difference  
423 in weight could also have different adverse effect when these particles are, for example,  
424 ingested by organisms. In addition, plastic emissions to the Oceans are estimate in weight [3]  
425 and determining MP weight could help for further estimation of MP source and quantities in  
426 the Oceans. In the present study, limit of detection of the optimized Py-GC/MS were  
427 estimated in  $\mu\text{g}$  because this technique is dependent on the particle weight and not their size.

428 Moreover, in other studies using thermal analyses, MP could be directly quantified in samples  
429 as previously demonstrated [22, 44]. Nevertheless, in the present study such quantification  
430 was not the purpose of the work. For further studies, MP weight should be estimated using  
431 weighting if possible or using volume calculation followed by weight estimation using a range  
432 of polymer density or using density found in the literature, as done by Simon et al, [43].

433 However, before being submitted to Py-GC/MS analysis, particles have to be handled with  
434 tweezers and placed in an analysis cup. The main limitation with the presented method is the  
435 “handibility” of the particles. Below 50  $\mu\text{m}$  it is very difficult to manipulate the particles as  
436 some particles may easily “fly away”. Here, the device is not the limiting element whereas the  
437 operator is as almost all theoretical identifiable sizes are below 50  $\mu\text{m}$ . Moreover, for  
438 application on unknown particles, the highest LOD have to be considered to ensure accurate  
439 identification. Consequently and to date, the effective lowest size for plastic identification  
440 with this Py-GC/MS method, using particle handling, was evaluated at 50  $\mu\text{m}$ .

441 Nevertheless, Py-GC/MS has been used to identify nanometric size scale plastic from bulk  
442 sample [31]. This approach was made possible as it did not use direct particles handling due  
443 to their sizes and because a data statistical treatment was applied after acquisition of  
444 pyrograms [31]. If direct handling of particles is not use, Py-GC/MS could be applied to  
445 identify smaller plastic particles. Indeed, the use of flow-cytometry using sorting [45] could  
446 be used to place potential MP in analysis cup. Flow cytometry in combination with a camera  
447 and a cell sorter have been used to detect MP [46]. Another technique could be the use of  
448 staining techniques like Nile red [47-49] before Py-GC/MS analysis. Indeed, stained particles  
449 could be introduced in analysis cup directly with the filter, for example. Moreover, the use of  
450 fixing solution to trap MP could also be a solution to isolate this particle and placing them in  
451 the analysis cup. However, potential interference of these solutions be carefully controlled

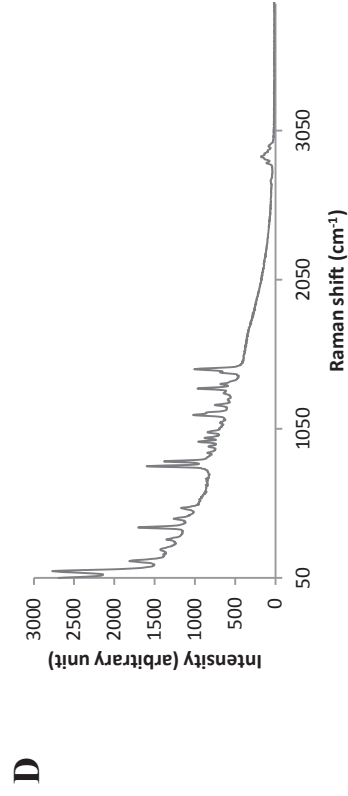
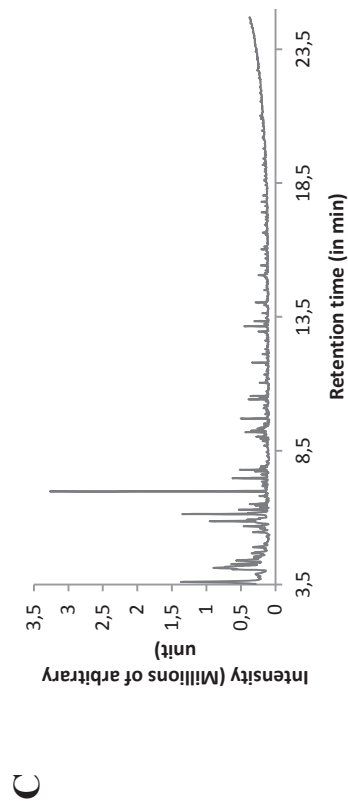
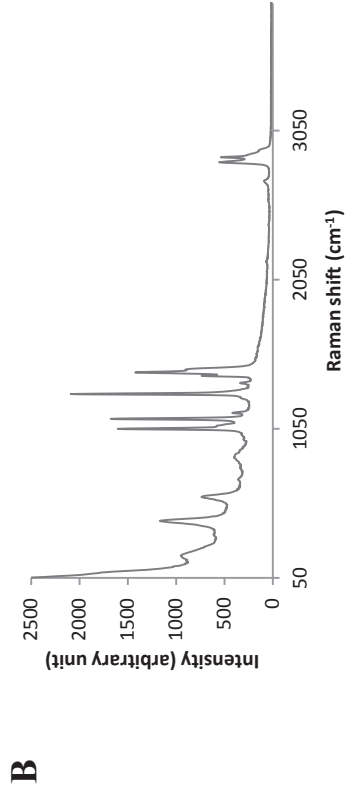
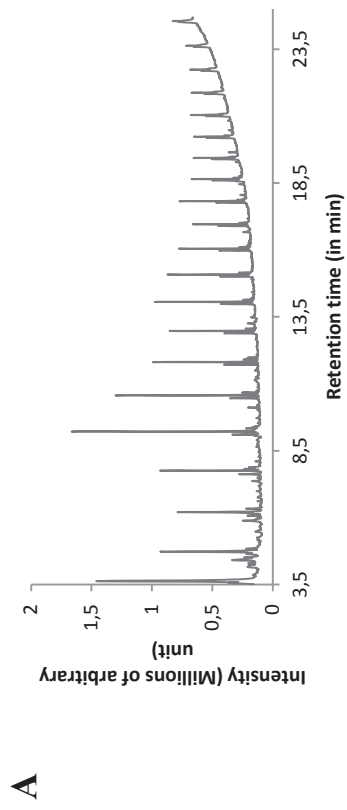
452 before to be employed in routine. With Py-GC/MS, development to isolate particles should be  
453 performed to enhance particle handling and to ensure that the device is the only limitation.

### 454 **3.3. Method comparison**

455 Here particles were collected by hand on a local beach. Particles used to compare  
456 identifications between  $\mu$ -Raman and Py-GC/MS were diverse in shapes and colors. The most  
457 common shape was fragments (21), followed by pellets (14), filaments (6), beads (5) and  
458 foams (4). Concerning particles color, green was the most common (8), followed by orange  
459 (7), blue (7), transparent (6), red (5), yellow (4), white (3), black (3), grey (3), purple (3), and  
460 pink (1).

461 Only forty out of fifty particles were identified with  $\mu$ -Raman as plastic particles. From the  
462 ten particles not identified, four were identified as pigments containing particles (Cobalt and  
463 copper phthalocyanine and Mortoperm blue). Among the 40 identified particles, there was:  
464 PE (22), PP (11), PS (3), PE-PP copolymer (3), and polyamide (1) (Fig 3).





465 Fig. 3 Pyrograms and Raman spectra acquired at 785 nm obtained from particles collected on a beach used for method comparison. Pyrogram and Raman spectra  
 466 respectively for a Polyethylene MP (A & B) and a Polypropylene MP (C & D).

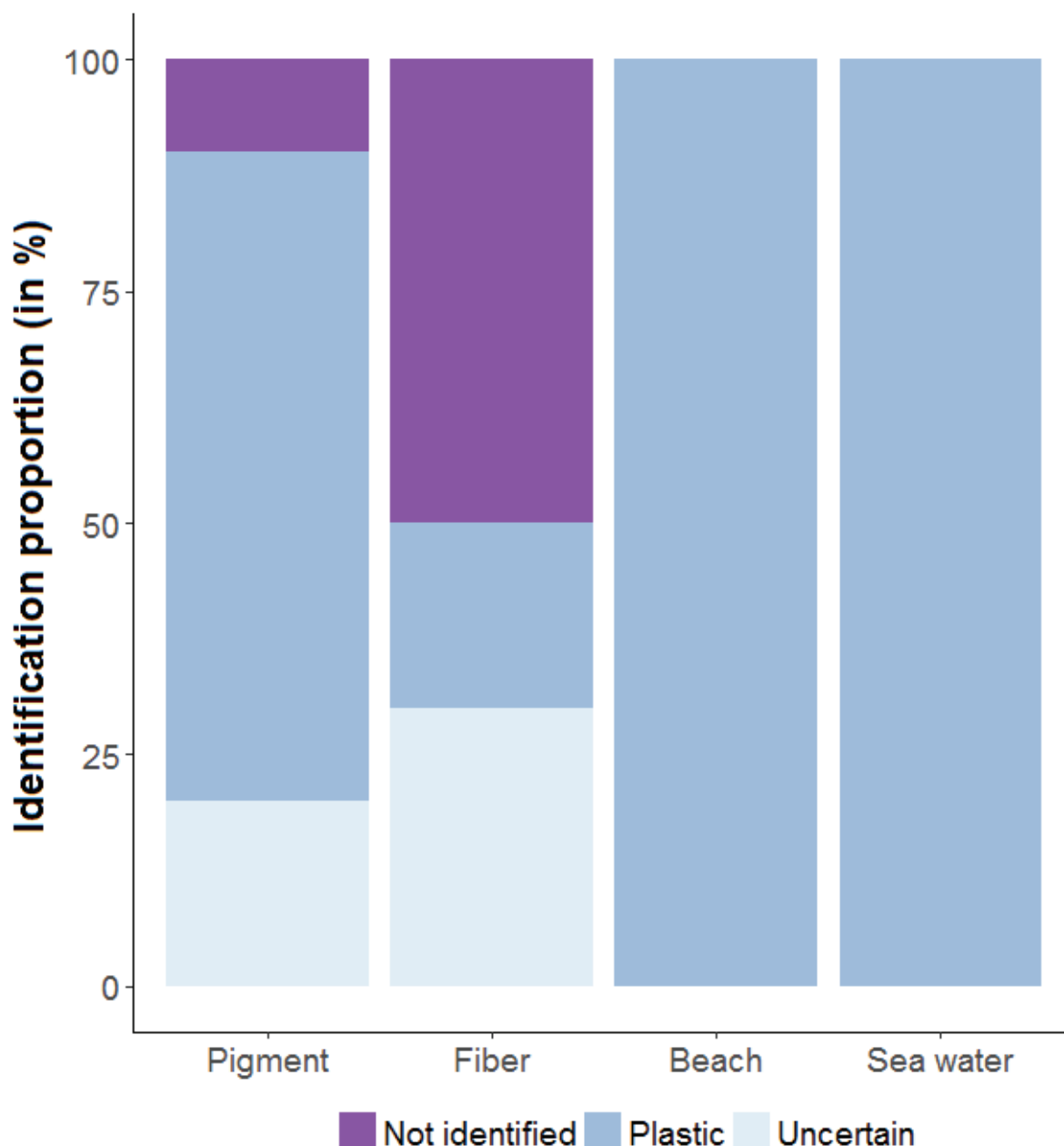
468 The optimized Py-GC/MS method also identified all the 40 particles. Thirty seven particles  
469 (92 %) were identified as they were after  $\mu$ -Raman analysis. Py-GC/MS led to results with a  
470 finer identification, two PP particles being identified as PE-PP copolymer. Moreover, the  
471 particle identified as polyamide with  $\mu$ -Raman was identified as a copolymer made of PE, PP  
472 and PA-6 (see Electronic Supplementary Material Figure S13). The optimized Py-GC/MS  
473 method identified 100 % of the 40 previously identified particles with  $\mu$ -Raman as plastic and  
474 demonstrated that this method is reliable for MP identification.

475 Some particles were not identified with  $\mu$ -Raman spectroscopy or were identified as  
476 pigments. Pigment containing particles identification were also obtained in previous studies  
477 on MP from water samples or marine organisms [16, 26-28]. Misidentification could occur for  
478 these pigmented particles pigments due to an overlaying of the polymer signal by the additive  
479 [11, 50]. Although some pigments are synthetic molecules, it could indicate a synthetic origin  
480 but those particles could not be classified as plastic with certainty leading to potential  
481 underestimation in field studies. Indeed some particle containing pigments could simply be  
482 colorful paint particles as demonstrated by Imhof et al, [50]. Out of the 6 not identified  
483 particles, 3 were discolored pellets. Discoloration indicates that pellets had a higher residence  
484 time in the environment [51]. Additionally, Py-GC/MS could also be complementary to FTIR  
485 to identified MP in field studies, as recently demonstrated [52]. Indeed, using FTIR polymer  
486 signal could be overlap by some plastic additives included and identification could be  
487 disturbed [53, 54]. In a recent study, Elert et al. [55] demonstrated that depending on the  
488 require information on MP information, *i.e.* quantification or identification of polymers, the  
489 appropriate technique should be used but the authors also indicated that identifications should  
490 be used in complementarity. Raman, FTIR and Py-GC/MS are, to date, the major  
491 identification techniques used in MP studies and those techniques are all complementary.

492 Then, the unidentified particles with  $\mu$ -Raman spectroscopy were analyzed by Py-GC/MS and  
493 included in the application section (*cf.* 3.4).

#### 494 **3.4. Application: identification of unknown particles**

495 On the sixty analyzed particles by Py-GC/MS, twenty (16 particles from bivalves and 4 from  
496 beach samples) formerly identified as pigment containing particles by  $\mu$ -Raman were  
497 processed by Py-GC/MS. All twenty particles were fragments with blue the dominant color  
498 with only one being green. Py-GC/MS identified 14 pigment particles as plastic polymers (70  
499 %), 4 pigment particles as plastic polymers with some uncertainty (20 %) and 2 particles were  
500 not identified (10% - Fig. 4). PS was the most common identified polymer (13 particles out of  
501 14) with one particle identified as a copolymer of PS and PMMA. Moreover, particles  
502 identified with uncertainty displayed characteristic compounds of PS but with low intensity.  
503 Here, Py-GC/MS identified 70 % of particles that were previously identified as pigment  
504 containing particles using  $\mu$ -Raman. Moreover,  $\mu$ -Raman only identified presence of the  
505 pigments nature as it overlaps with polymer signals, while Pyrolysis only allow to identify the  
506 native plastic polymer. Despite an effective lowest size of 50  $\mu\text{m}$ , due to handling issue, being  
507 10 to 50 times higher than the lowest size respectively analyzable by FTIR or  $\mu$ -Raman  
508 spectroscopy, respectively, the Py-GC/MS method is still competitive and complementary.  
509 Indeed, as it allows (i) the full identification of pigments and some fibers and (ii) could be  
510 combined with improved separation methods to retrieve smaller particles. Here, Py-GC/MS  
511 could be used as a complementary identification method after  $\mu$ -Raman spectroscopy.



512  
 513 **Fig. 4** Sample proportion for each identification class obtained after Py-GC/MS for particles previously  
 514 identified as pigment (n=20) by  $\mu$  Raman, fibers (n=10) and particles collected on a beach (n=6) and in  
 515 surface sea water of the Bay of Brest (n=24). Not identified correspond to particles with low or no  
 516 discernible signal, Uncertain to identification as plastic with some uncertainty and Plastic to identification  
 517 with accurate polymer attribution

518 Out of the 10 fibers extracted from bivalves, 7 were blue, 2 were black, and 1 was red. For  
 519 fibers, identification was achieved having 2 fibers identified as PE and Polyacrylonitrile  
 520 (PAN). Fibers made of PAN, PE and potentially PET were identify and such polymer are  
 521 commonly used in the textile industry [56] and are found in wastewater treatment plants after  
 522 washing machine [57]. Three fibers were identified as plastic polymer with some uncertainty

523 and 5 fibers were not identified due to low or absent signal (Fig. 5). Uncertain identification  
524 for fibers comprised 1 PE and 2 PET. Fibers identification was tough. Indeed, only 20 % of  
525 the analyzed fibers were correctly identified. As fibers are long and thin, they are lighter in  
526 comparison with fragment. As Py-GC/MS rely more on particle weight than on their size, low  
527 weight could result in uncertainty with identifications, as previously observed for fibers in a  
528 study conducted by [Hendrickson et al, \[24\]](#). To improve fibers and small particles  
529 identification, a solution could be the use of single ion monitoring (SIM) which target selected  
530 ion (m/z) allowing to decrease the LOD.

531 Out of the 30 others particles collected at sea-surface or in beach sediment, fragments (10)  
532 were the most common particles followed by foams (6), filaments (5), pellets (4), films (4),  
533 and beads (1). Regarding particles color: white was the dominant color (8) followed by blue  
534 (6), orange (5), transparent (5), green (3), red (1), black (1), and yellow (1). Particles were all  
535 identified as plastic with no uncertainty (Fig. 5) however it is important to indicate that the  
536 particule used in this section were large MP cut (*ca.* 200  $\mu\text{m}$ ) to be introduced in an analysis  
537 cup. PE (14) was the most common polymer followed by PP (9) and PS (4). Other polymers  
538 including PE-PP copolymer, Chlorinated PE (CPE), and Acrylonitrile-butadiene-styrene  
539 copolymer (ABS) were each found only once. Py-GC/MS provide good identification with  
540 similarity percentage above 80 %. The differentiation between PS and ABS remained difficult  
541 as both polymers are made with styrene which is the major characteristic compounds of their  
542 pyrograms [32, 33]. ABS reference presented an interesting characteristic compound: 1-  
543 Naphthalenecarbonitrile. This compound was only present in ABS reference pyrogram.  
544 Differentiation was made using this compound and tracking it in the pyrogram using its major  
545 ion: 153 m/z. Polymers identified *i.e.* PE, PP and PS are commonly reported on the beach [58]  
546 and in sea-surface water [38].

#### 547 **4. Conclusion**

548 The present work described an in-depth optimization of a Py-GC/MS method to identify MP  
549 followed by an efficiency assessment of its performance and a comparison with Raman  
550 spectroscopic approach. In addition, to evaluate the robustness of the optimized Py-GC/MS  
551 method to identify MP, it was applied on samples from different matrices: bivalve, beach and  
552 sea-water surface. Optimization demonstrated that increasing pyrolysis temperature up to 700  
553 °C in combination with a split ratio of 5 and an injector temperature set at 300 °C improved  
554 signal detection. Then, performance assessment demonstrated that if signal vary over time,  
555 such variation had no impact on MP identification. This method is validated on qualitative  
556 data but not on quantitative one due to RSD value above 20 % for repeatability and  
557 intermediate precision.

558 The optimized Py-GC/MS has some advantages in comparison with other MP identification  
559 methods. Firstly, Py-GC/MS is a complementary method to spectroscopy approaches. Indeed,  
560 in the present study Py-GC/MS enable identification of pigment containing particles right  
561 after  $\mu$ -Raman analysis. Moreover Py-GC/MS identified co-polymer like PE-PP or PE-PP-  
562 PA6 which could be difficult to identify with  $\mu$ -Raman without chemometrics approach.  
563 Secondly, up to date, Py-GC/MS identification of plastic particles cannot be done below 50  
564  $\mu\text{m}$  (longest size) not because of LOD but due to operator handling issues. A better way, like  
565 the introduction of a piece of filter on which particles are into the analysis cup, should be  
566 developed in order to avoid this limiting step. However, Py-GC/MS could be used to identify  
567 smaller particles, like nanoplastics as already demonstrated. By resolving this handling issue,  
568 LOD calculation demonstrated that this method could identify isolated MP weighting below 1  
569  $\mu\text{g}$ . In addition, another strategy that can be considered to lower the LOD for this Py-GC/MS  
570 method is the use of SIM. To get identification on MP polluting from both freshwater and  
571 marine environment, the use of Py-GC/MS should be better considered as this method prove

572 to be efficient in identifying MP from various matrices. In an effort to standardize the MP  
573 analysis workflow, this method could be implemented either on its own or after FTIR or  
574 Raman to confirm some identification or to circumvent unsuccessful spectroscopy  
575 identification. Finally, MP mass should be evaluated in MP studies to try to standardized  
576 leading to better comparison of MP contamination between studies.

577

## 578 **Acknowledgments**

579 Ludovic Hermabessiere is grateful to the Hauts-de-France Region and ANSES (French  
580 Agency for Food, Environmental and Occupational Health & Safety) for the financial support  
581 of his PhD. Maria Kazour is financially supported by a PhD fellowship from the National  
582 Council for Scientific Research (Lebanon) and Université du Littoral Côte d'Opale (France).  
583 This paper has been funded by the French National Research Agency (ANR) (ANR-15-CE34-  
584 0006-02), as part of the Nanoplastics project and also by the French government and the  
585 Hauts-de-France Region in the framework of the project CPER 2014-2020 MARCO.

586 This is a post-peer-review, pre-copyedit version of an article published in Analytical and  
587 Bioanalytical Chemistry. The final authenticated version is available online at:  
588 <https://doi.org/10.1007/s00216-018-1279-0>

## 589 **Compliance with Ethical Standards**

590 Conflict of Interest: Authors declare no conflict of interest.

## 591 **References**

- 592 1. Thompson, R.C., S.H. Swan, C.J. Moore, and F.S. vom Saal, 2009. Our plastic age.  
593 Philosophical Transactions of the Royal Society B: Biological Sciences. 364, 1973-  
594 1976. doi: 10.1098/rstb.2009.0054
- 595 2. PlasticsEurope, 2018. Plastics – the Facts 2017: An analysis of European plastics  
596 production, demand and waste data. Available on:  
597 <http://www.plasticseurope.fr/Document/plastics---the-facts-2017.aspx?FolID=2>,  
598 Accessed on: 01/29/2018
- 599 3. Jambeck, J.R., R. Geyer, C. Wilcox, T.R. Siegler, M. Perryman, A. Andrady, R.  
600 Narayan, and K.L. Law, 2015. Plastic waste inputs from land into the ocean. Science.  
601 347, 768-771. doi: 10.1126/science.1260352
- 602 4. Cózar, A., F. Echevarría, J.I. González-Gordillo, X. Irigoien, B. Úbeda, S. Hernández-  
603 León, Á.T. Palma, S. Navarro, J. García-de-Lomas, A. Ruiz, M.L. Fernández-de-  
604 Puellas, and C.M. Duarte, 2014. Plastic debris in the open ocean. Proceedings of the  
605 National Academy of Sciences. 111, 10239-10244. doi: 10.1073/pnas.1314705111
- 606 5. Eriksen, M., L.C. Lebreton, H.S. Carson, M. Thiel, C.J. Moore, J.C. Borerro, F.  
607 Galgani, P.G. Ryan, and J. Reisser, 2014. Plastic pollution in the world's oceans: more



- 608 than 5 trillion plastic pieces weighing over 250,000 tons afloat at sea. PloS one. 9,  
609 e111913.
- 610 6. van Sebille, E., C. Wilcox, L. Lebreton, N. Maximenko, B.D. Hardesty, J.A. van  
611 Franeker, M. Eriksen, D. Siegel, F. Galgani, and K.L. Law, 2015. A global inventory  
612 of small floating plastic debris. Environmental Research Letters. 10, 124006.
- 613 7. Arthur, C., J. Baker, and H. Bamford, 2009. International Research Workshop on the  
614 Occurrence, Effects, and Fate of Microplastic Marine Debris. NOAA Technical  
615 Memorandum NOS-OR&R-30.
- 616 8. Li, W.C., H.F. Tse, and L. Fok, 2016. Plastic waste in the marine environment: A  
617 review of sources, occurrence and effects. Science of The Total Environment. 566–  
618 567, 333-349. doi: 10.1016/j.scitotenv.2016.05.084
- 619 9. Horton, A.A., A. Walton, D.J. Spurgeon, E. Lahive, and C. Svendsen, 2017.  
620 Microplastics in freshwater and terrestrial environments: Evaluating the current  
621 understanding to identify the knowledge gaps and future research priorities. Science of  
622 The Total Environment. 586, 127-141. doi: 10.1016/j.scitotenv.2017.01.190
- 623 10. Imhof, H.K., J. Schmid, R. Niessner, N.P. Ivleva, and C. Laforsch, 2012. A novel,  
624 highly efficient method for the separation and quantification of plastic particles in  
625 sediments of aquatic environments. Limnology and Oceanography: Methods. 10, 524-  
626 537. doi: 10.4319/lom.2012.10.524
- 627 11. Lenz, R., K. Enders, C.A. Stedmon, D.M.A. Mackenzie, and T.G. Nielsen, 2015. A  
628 critical assessment of visual identification of marine microplastic using Raman  
629 spectroscopy for analysis improvement. Marine Pollution Bulletin. 100, 82-91. doi:  
630 10.1016/j.marpolbul.2015.09.026
- 631 12. Shim, W.J., S.H. Hong, and S.E. Eo, 2017. Identification methods in microplastic  
632 analysis: a review. Analytical Methods. 9, 1384-1391. doi: 10.1039/C6AY02558G
- 633 13. CAMPUS, 2018. Available on: <https://www.campusplastics.com/campus/list>,  
634 Accessed on: 01/26/2018
- 635 14. Remy, F., F. Collard, B. Gilbert, P. Compère, G. Eppe, and G. Lepoint, 2015. When  
636 Microplastic Is Not Plastic: The Ingestion of Artificial Cellulose Fibers by  
637 Macrofauna Living in Seagrass Macrophytodetritus. Environmental Science &  
638 Technology. 49, 11158-11166. doi: 10.1021/acs.est.5b02005
- 639 15. Rocha-Santos, T. and A.C. Duarte, 2015. A critical overview of the analytical  
640 approaches to the occurrence, the fate and the behavior of microplastics in the  
641 environment. Trends in Analytical Chemistry. 65, 47-53. doi:  
642 10.1016/j.trac.2014.10.011
- 643 16. Frère, L., I. Paul-Pont, J. Moreau, P. Soudant, C. Lambert, A. Huvet, and E. Rinnert,  
644 2016. A semi-automated Raman micro-spectroscopy method for morphological and  
645 chemical characterizations of microplastic litter. Marine Pollution Bulletin. 113, 461-  
646 468. doi: 10.1016/j.marpolbul.2016.10.051
- 647 17. Oßmann, B.E., G. Sarau, S.W. Schmitt, H. Holtmannspötter, S.H. Christiansen, and  
648 W. Dicke, 2017. Development of an optimal filter substrate for the identification of  
649 small microplastic particles in food by micro-Raman spectroscopy. Analytical and  
650 Bioanalytical Chemistry. 409, 4099-4109. doi: 10.1007/s00216-017-0358-y
- 651 18. Phuong, N.N., A. Zalouk-Vergnoux, A. Kamari, C. Mouneyrac, F. Amiard, L. Poirier,  
652 and F. Lagarde, 2017. Quantification and characterization of microplastics in blue  
653 mussels (*Mytilus edulis*): protocol setup and preliminary data on the contamination of  
654 the French Atlantic coast. Environmental Science and Pollution Research, 1-10. doi:  
655 10.1007/s11356-017-8862-3

- 656 19. Dekiff, J.H., D. Remy, J. Klasmeier, and E. Fries, 2014. Occurrence and spatial  
657 distribution of microplastics in sediments from Norderney. *Environmental Pollution*.  
658 186, 248-256. doi: 10.1016/j.envpol.2013.11.019
- 659 20. Fries, E., J.H. Dekiff, J. Willmeyer, M.-T. Nuelle, M. Ebert, and D. Remy, 2013.  
660 Identification of polymer types and additives in marine microplastic particles using  
661 pyrolysis-GC/MS and scanning electron microscopy. *Environmental Science:  
662 Processes & Impacts*. 15, 1949-1956. doi: 10.1039/C3EM00214D
- 663 21. Nuelle, M.-T., J.H. Dekiff, D. Remy, and E. Fries, 2014. A new analytical approach  
664 for monitoring microplastics in marine sediments. *Environmental Pollution*. 184, 161-  
665 169. doi: 10.1016/j.envpol.2013.07.027
- 666 22. Fischer, M. and B.M. Scholz-Böttcher, 2017. Simultaneous Trace Identification and  
667 Quantification of Common Types of Microplastics in Environmental Samples by  
668 Pyrolysis-Gas Chromatography–Mass Spectrometry. *Environmental Science &  
669 Technology*. 51, 5052-5060. doi: 10.1021/acs.est.6b06362
- 670 23. Fabbri, D., D. Tartari, and C. Trombini, 2000. Analysis of poly(vinyl chloride) and  
671 other polymers in sediments and suspended matter of a coastal lagoon by pyrolysis-  
672 gas chromatography-mass spectrometry. *Analytica Chimica Acta*. 413, 3-11. doi:  
673 10.1016/S0003-2670(00)00766-2
- 674 24. Hendrickson, E., E.C. Minor, and K. Schreiner, 2018. Microplastic abundance and  
675 composition in western Lake Superior as determined via microscopy, Pyr-GC/MS, and  
676 FTIR. *Environmental Science & Technology*. 52, 1787-1796. doi:  
677 10.1021/acs.est.7b05829
- 678 25. Ceccarini, A., A. Corti, F. Erba, F. Modugno, J. La Nasa, S. Bianchi, and V.  
679 Castelvetro, 2018. The hidden microplastics. New insights and figures from the  
680 thorough separation and characterization of microplastics and of their degradation by-  
681 products in coastal sediments. *Environmental Science & Technology*. doi:  
682 10.1021/acs.est.8b01487
- 683 26. Van Cauwenberghe, L., M. Claessens, M.B. Vandegehuchte, and C.R. Janssen, 2015.  
684 Microplastics are taken up by mussels (*Mytilus edulis*) and lugworms (*Arenicola  
685 marina*) living in natural habitats. *Environmental Pollution*. 199, 10-17. doi:  
686 10.1016/j.envpol.2015.01.008
- 687 27. Van Cauwenberghe, L. and C.R. Janssen, 2014. Microplastics in bivalves cultured for  
688 human consumption. *Environmental Pollution*. 193, 65-70. doi:  
689 10.1016/j.envpol.2014.06.010
- 690 28. Schymanski, D., C. Goldbeck, H.-U. Humpf, and P. Fürst, 2018. Analysis of  
691 microplastics in water by micro-Raman spectroscopy: Release of plastic particles from  
692 different packaging into mineral water. *Water Research*. 129, 154-162. doi:  
693 10.1016/j.watres.2017.11.011
- 694 29. Li, J., H. Liu, and J. Paul Chen, 2018. Microplastics in freshwater systems: A review  
695 on occurrence, environmental effects, and methods for microplastics detection. *Water  
696 Research*. 137, 362-374. doi: 10.1016/j.watres.2017.12.056
- 697 30. Ivleva, N.P., A.C. Wiesheu, and R. Niessner, 2016. Microplastic in Aquatic  
698 Ecosystems. *Angewandte Chemie International Edition*. 56, 1720-1739. doi:  
699 10.1002/anie.201606957
- 700 31. Ter Halle, A., L. Jeanneau, M. Martignac, E. Jardé, B. Pedrono, L. Brach, and J.  
701 Gigault, 2017. Nanoplastic in the North Atlantic Subtropical Gyre. *Environmental  
702 Science & Technology*. 51, 13689-13697. doi: 10.1021/acs.est.7b03667
- 703 32. Tsuge, S., H. Ohtani, and C. Watanabe, *Pyrolysis-GC/MS Data Book of Synthetic  
704 Polymers*. 2011: Elsevier. 390.

- 705 33. Kusch, P., *Application of Pyrolysis-Gas Chromatography/Mass Spectrometry (Py-*  
706 *GC/MS)*, in *Characterization and Analysis of Microplastics*, T. Rocha-Santos and A.  
707 Duarte, Editors. 2016, Elsevier. p. 306.
- 708 34. van Den Dool, H. and P.D. Kratz, 1963. A generalization of the retention index system  
709 including linear temperature programmed gas—liquid partition chromatography.  
710 *Journal of Chromatography A*. 11, 463-471. doi: 10.1016/S0021-9673(01)80947-X
- 711 35. Dehaut, A., A.-L. Cassone, L. Frère, L. Hermabessiere, C. Himber, E. Rinnert, G.  
712 Rivière, C. Lambert, P. Soudant, A. Huvet, G. Duflos, and I. Paul-Pont, 2016.  
713 *Microplastics in seafood: Benchmark protocol for their extraction and*  
714 *characterization. Environmental Pollution*. 215, 223-233. doi:  
715 10.1016/j.envpol.2016.05.018
- 716 36. International Organization for Standardization (ISO), 1994. 5725-3: 1994, Accuracy  
717 (trueness and precision) of measurement methods and results-Part 3: Intermediate  
718 measures of the precision of a standard measurement method. International  
719 Organization for Standardization, Geneva.
- 720 37. Caporal-Gautier, J., M. Nivet J, P. Algranti, M. Guilloteau, M. Histe, M. Lallier, J.  
721 N'Guyen-Huu J, and R. Russotto, 1992. Guide de validation analytique. Rapport d'une  
722 commission SFSTP. I : Méthodologie. STP pharma pratiques. 2, 205-226.
- 723 38. Frère, L., I. Paul-Pont, E. Rinnert, S. Petton, J. Jaffré, I. Bihannic, P. Soudant, C.  
724 Lambert, and A. Huvet, 2017. Influence of environmental and anthropogenic factors  
725 on the composition, concentration and spatial distribution of microplastics: A case  
726 study of the Bay of Brest (Brittany, France). *Environmental Pollution*. 225, 211-222.  
727 doi: <https://doi.org/10.1016/j.envpol.2017.03.023>
- 728 39. R Core Team, 2015. R: A language and environment for statistical computing. Vienna,  
729 Austria; 2014. Available on: <http://www.R-project.org>, Accessed on: 10/15/2015
- 730 40. De Mendiburu, F., 2014. *Agricolae: statistical procedures for agricultural research*. R  
731 package version.
- 732 41. McGuffin, V.L., *Theory of chromatography*, in *Journal of Chromatography Library*.  
733 2004, Elsevier. p. 1-93.
- 734 42. Filella, M., 2015. Questions of size and numbers in environmental research on  
735 microplastics: methodological and conceptual aspects. *Environmental Chemistry*. 12,  
736 527-538. doi: 10.1071/EN15012
- 737 43. Simon, M., N. van Alst, and J. Vollertsen, 2018. Quantification of microplastic mass  
738 and removal rates at wastewater treatment plants applying Focal Plane Array (FPA)-  
739 based Fourier Transform Infrared (FT-IR) imaging. *Water Research*. 142, 1-9. doi:  
740 10.1016/j.watres.2018.05.019
- 741 44. Dümichen, E., A.-K. Barthel, U. Braun, C.G. Bannick, K. Brand, M. Jekel, and R.  
742 Senz, 2015. Analysis of polyethylene microplastics in environmental samples, using a  
743 thermal decomposition method. *Water Research*. 85, 451-457. doi:  
744 10.1016/j.watres.2015.09.002
- 745 45. Ibrahim, S.F. and G. van den Engh, *Flow Cytometry and Cell Sorting*, in *Cell*  
746 *Separation: Fundamentals, Analytical and Preparative Methods*, A. Kumar, I.Y.  
747 Galaev, and B. Mattiasson, Editors. 2007, Springer Berlin Heidelberg: Berlin,  
748 Heidelberg. p. 19-39.
- 749 46. Sgier, L., R. Freimann, A. Zupanic, and A. Kroll, 2016. Flow cytometry combined  
750 with viSNE for the analysis of microbial biofilms and detection of microplastics.  
751 *Nature communications*. 7, 11587.
- 752 47. Shim, W.J., Y.K. Song, S.H. Hong, and M. Jang, 2016. Identification and  
753 quantification of microplastics using Nile Red staining. *Marine Pollution Bulletin*.  
754 113, 469-476. doi: 10.1016/j.marpolbul.2016.10.049

- 755 48. Maes, T., R. Jessop, N. Wellner, K. Haupt, and A.G. Mayes, 2017. A rapid-screening  
756 approach to detect and quantify microplastics based on fluorescent tagging with Nile  
757 Red. *Scientific Reports*. 7, 44501. doi: 10.1038/srep44501
- 758 49. Erni-Cassola, G., M.I. Gibson, R.C. Thompson, and J.A. Christie-Oleza, 2017. Lost,  
759 but Found with Nile Red: A Novel Method for Detecting and Quantifying Small  
760 Microplastics (1 mm to 20  $\mu$ m) in Environmental Samples. *Environmental Science &*  
761 *Technology*. 51, 13641-13648. doi: 10.1021/acs.est.7b04512
- 762 50. Imhof, H.K., C. Laforsch, A.C. Wiesheu, J. Schmid, P.M. Anger, R. Niessner, and  
763 N.P. Ivleva, 2016. Pigments and plastic in limnetic ecosystems: A qualitative and  
764 quantitative study on microparticles of different size classes. *Water Research*. 98, 64-  
765 74. doi: 10.1016/j.watres.2016.03.015
- 766 51. Endo, S., R. Takizawa, K. Okuda, H. Takada, K. Chiba, H. Kanehiro, H. Ogi, R.  
767 Yamashita, and T. Date, 2005. Concentration of polychlorinated biphenyls (PCBs) in  
768 beached resin pellets: Variability among individual particles and regional differences.  
769 *Marine Pollution Bulletin*. 50, 1103-1114. doi: 10.1016/j.marpolbul.2005.04.030
- 770 52. Kappler, A., M. Fischer, B.M. Scholz-Bottcher, S. Oberbeckmann, M. Labrenz, D.  
771 Fischer, K.-J. Eichhorn, and B. Voit, 2018. Comparison of  $\mu$ -ATR-FTIR spectroscopy  
772 and py-GCMS as identification tools for microplastic particles and fibers isolated from  
773 river sediments. *Analytical and Bioanalytical Chemistry*. doi: 10.1007/s00216-018-  
774 1185-5
- 775 53. Tabb, D.L. and J.L. Koenig, 1975. Fourier Transform Infrared Study of Plasticized  
776 and Unplasticized Poly(vinyl chloride). *Macromolecules*. 8, 929-934. doi:  
777 10.1021/ma60048a043
- 778 54. Gonzalez, N. and M.J. Fernandez-Berridi, 2006. Application of Fourier transform  
779 infrared spectroscopy in the study of interactions between PVC and plasticizers:  
780 PVC/plasticizer compatibility versus chemical structure of plasticizer. *Journal of*  
781 *Applied Polymer Science*. 101, 1731-1737. doi: doi:10.1002/app.23381
- 782 55. Elert, A.M., R. Becker, E. Duemichen, P. Eisentraut, J. Falkenhagen, H. Sturm, and U.  
783 Braun, 2017. Comparison of different methods for MP detection: What can we learn  
784 from them, and why asking the right question before measurements matters?  
785 *Environmental Pollution*. 231, 1256-1264. doi: 10.1016/j.envpol.2017.08.074
- 786 56. Napper, I.E. and R.C. Thompson, 2016. Release of synthetic microplastic plastic  
787 fibres from domestic washing machines: Effects of fabric type and washing  
788 conditions. *Marine Pollution Bulletin*. 112, 39-45. doi:  
789 <https://doi.org/10.1016/j.marpolbul.2016.09.025>
- 790 57. Browne, M.A., P. Crump, S.J. Niven, E. Teuten, A. Tonkin, T. Galloway, and R.  
791 Thompson, 2011. Accumulation of Microplastic on Shorelines Worldwide: Sources  
792 and Sinks. *Environmental Science & Technology*. 45, 9175-9179. doi:  
793 10.1021/es201811s
- 794 58. Lots, F.A.E., P. Behrens, M.G. Vijver, A.A. Horton, and T. Bosker, 2017. A large-  
795 scale investigation of microplastic contamination: Abundance and characteristics of  
796 microplastics in European beach sediment. *Marine Pollution Bulletin*. 123, 219-226.  
797 doi: <https://doi.org/10.1016/j.marpolbul.2017.08.057>

798